Optical Millimeter-Wave Up-Conversion Employing Frequency Quadrupling Without Optical Filtering

Chun-Ting Lin, Po-Tsung Shih, Jason (Jyehong) Chen, Wen-Jr Jiang, Sheng-Peng Dai, Peng-Chun Peng, Yen-Lin Ho, and Sien Chi

***Abstract*—This study presents two optical frequency quadrupling techniques for generating high-purity millimeter-wave signals with optical carrier suppression. To our best knowledge, this investigation demonstrates for the first time that a frequency quadrupling system requires only a single integrated Mach–Zehnder modulator without an optical narrowband filter to remove undesired optical sidebands. Since no optical filter is needed, fast frequency tuning is straightforward and this approach is particularly attractive for the optical up-conversion in the wavelength-division-multiplexing radio-over-fiber systems. This study provides both theoretical analysis and experimental demonstration. The generated optical millimeter-wave signals are of very high quality with optical carrier and undesired harmonic distortion suppression ratio of more than 36 dB.**

***Index Terms*—Mach–Zehnder modulator (MZM), optical frequency multiplication, optical millimeter wave, radio-over-fiber (RoF).**

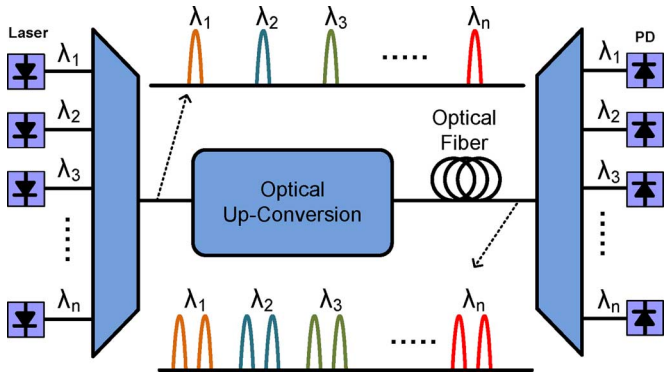

Fig. 1. Optical colorless up-conversion using a frequency multiplication technique for WDM RoF systems.

I. Introduction

With the accelerated development of wireless communications, efficient and cost-effective methods of generating and transmitting microwave/millimeter-wave signals are of the utmost importance. The generation and transmission of microwave/millimeter-wave signals over an optical fiber have been extensively investigated for various applications, including broadband wireless access networks, phase-array antennas, optical sensors, remote antenna, and radars [1]–[7]. The advantages of using an optical fiber as a millimeter-wave signal transmission medium lie in the almost unlimited bandwidth and very low propagation loss. However, optical millimeter-wave signal generation at frequencies beyond 40 GHz remains a major challenge because of the frequency response of an $LiNbO_3$ Mach–Zehnder modulator (MZM) or a phase modulator is less than 40 GHz. The electrical components and equipment at frequencies beyond 40 GHz, such as amplifiers, mixers, and synthesizers, are very expensive. Therefore, a cost-effective means of generating optical millimeter-wave signal beyond 40 GHz is of great interest.

Several optical millimeter-wave signal generation schemes based on an MZM or a phase modulator to achieve frequency multiplication have recently been demonstrated [1]–[10]. However, these proposed systems with frequency multiplication of more than two times either depend on more than one optical filter to remove undesired optical sidebands [2]–[10] or need two cascaded external modulators [13], which significantly increase the complexity and cost of the system. Besides, the required optical filtering severely hinders the implementation of optical up-conversion in a wavelength-division-multiplexer (WDM) radio-over-fiber (RoF) system, as shown in Fig. 1. Although one external modulator with optical filtering is utilized to demonstrate WDM up-conversion in [11], only frequency doubling is achieved.

This study demonstrates the feasibility of two novel frequency quadrupling approaches that can generate optical carrier-suppressed millimeter-wave signals using only one external modulator without optical filtering. The first method sets the bias point of the MZM at the maximum transmission point, which has been proposed in our previous study [14]. More experimental data, including higher undesired harmonic distortion suppression ratio and millimeter-wave signal beyond 40 GHz, will be given in this paper. The second approach changes the bias point to the minimum transmission point. The optical carrier and undesired harmonic distortion suppression ratios (OCHDSRs) of the millimeter-wave signals obtained using maximum and minimum transmission operation modes exceed 36 and 20 dB, respectively. Since the optical carrier

Manuscript received June 03, 2008; revised October 25, 2008. First published July 07, 2009; current version published August 12, 2009. This work was supported by the National Science Council, Taiwan under Contract NSC 96-2221-E-155-038-MY2, Contract NSC 96-2752-E-009-004-PAE, and Contract NSC 96-2628-E-009-016.

C.-T. Lin is with the Institute of Photonic System, College of Photonics, National Chiao Tung University at Tainan, Taiwan 71150 (e-mail: jintingtw@gmail.com).

P.-T. Shih, J. Chen, W.-J. Jiang, S.-P. Dai, and Y.-L. Ho are with the Department of Photonics, National Chiao Tung University, Hsinchu 300, Taiwan.

P.-C. Peng is with the Department of Electro-Optical Engineering, National Taipei University of Technology, Taipei 10608, Taiwan.

S. Chi is with the Department of Electrical Engineering, Yuan Ze University, Jung-Li, TaoYuan 320, Taiwan.

Color versions of one or more of the figures in this paper are available online at http://ieeexplore.ieee.org

Digital Object Identifier 10.1109/TMTT.2009.2015036

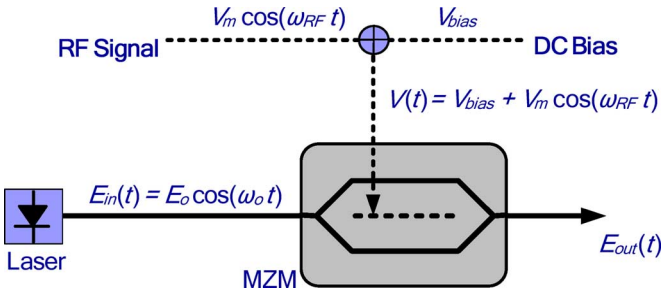

Fig. 2. Principle diagram of optical millimeter-wave generation using external MZM.

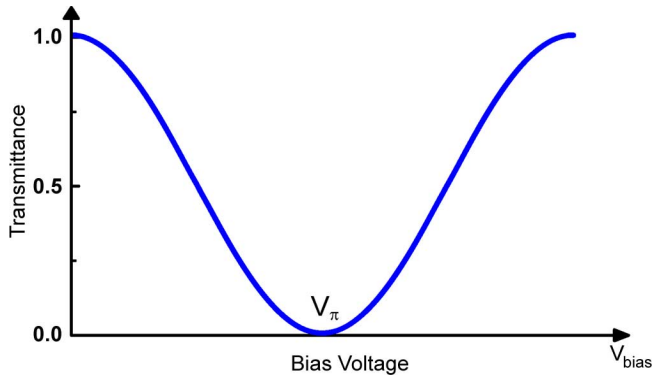

Fig. 3. Transmission function of MZM versus bias voltage.

and undesired harmonic distortions are highly suppressed, the high-purity two-tone millimeter-wave signal does not suffer from impairment due to fiber dispersion. This paper is organized as follows. Section II presents theoretical analyses of optical quadruple-frequency millimeter-wave signal generations obtained using maximum and minimum transmission operation modes. In Section III, optical 40- and 72-GHz millimeter-wave signals using electrical 10- and 18-GHz driving signals are experimentally demonstrated. Section IV shows the comparison of two proposed methods. Conclusions and summary are finally drawn in Section V.

II. Theoretical Analysis

A. Principle of MZM Modulation

Fig. 2 displays the principle of the optical millimeter-wave signal generation using a balanced single-electrode MZM. The driving signal $V(t)$ sent to the MZM consists of an electrical sinusoidal signal and a dc-biased voltage and can be written as

$$V(t) = V_{\text{bias}} + V_m \cos(\omega_{\text{RF}} t) \tag{1}$$

where V_{bias} is the dc-bias voltage, and V_m and ω_{RF} are the amplitude and the angular frequency of the electrical driving signal, respectively. It is known that the optical field at the output of the MZM is given by

$$E_{\text{out}}(t) = E_o \cos\left[\frac{\Phi\left[V(t)\right]}{2}\right] \cos(\omega_o t) \tag{2}$$

where E_o and ω_o denote the amplitude and angular frequency of the input optical carrier, respectively, and $\Phi[V(t)]$ is the optical carrier phase difference that is induced by $V(t)$ between the two arms of the MZM. The loss of the MZM is neglected. The optical carrier phase difference induced by $V(t)$ is given by

$$\Phi\left[V(t)\right] = \pi\left[\frac{V_{\text{bias}}}{V_\pi} + \frac{V_m}{V_\pi}\cos(\omega_{\text{RF}} t)\right] \tag{3}$$

where V_π is the half-wave voltage of the MZM. Therefore, the output optical field can be expressed as

$$E_{\text{out}}(t) = E_o \cos\left(\frac{\pi}{2}\left[\frac{V_{\text{bias}}}{V_\pi} + \frac{V_m}{V_\pi}\cos(\omega_{\text{RF}} t)\right]\right)\cos(\omega_o t). \tag{4}$$

Expanding (4) using Bessel functions, the optical field at the output of the MZM can be rewritten as

$$\begin{aligned} E_{\text{out}}(t) = & E_o \cos b \\ & \cdot \Bigg\{ J_o(m)\cos(\omega_o t) \\ & \quad + \sum_{n=1}^{\infty} [J_{2n}(m)\cos(\omega_o t + 2n\omega_{\text{RF}} t - n\pi) \\ & \qquad + J_{2n}(m)\cos(\omega_o t - 2n\omega_{\text{RF}} t + n\pi)] \Bigg\} \\ & + E_o \sin b \\ & \cdot \Bigg\{ \sum_{n=1}^{\infty} [J_{2n-1}(m)\cos(\omega_o t + (2n-1)\omega_{\text{RF}} t - n\pi) \\ & \qquad + J_{2n-1}(m)\cos(\omega_o t - (2n-1)\omega_{\text{RF}} t + n\pi)] \Bigg\} \end{aligned} \tag{5}$$

where $b = (V_{\text{bias}}/2V_\pi)\pi$ is a constant phase shift that is induced by the MZM biased voltage, m is defined as $(V_m/2V_\pi)\pi$, and J_n is the Bessel function of the first kind of order n. Notably, the MZM bias point affects the relative amplitudes of odd and even terms of optical sidebands.

Fig. 3 shows MZM transmittance versus the bias voltage. As the MZM is operated at the maximum transmission point (i.e., $V_{\text{bias}} = 0$ or $b = 0$), only optical carrier and even terms of optical sidebands are observed and no odd terms of optical sidebands exist, as shown in Fig. 4(a). As the MZM is biased at the minimum transmission point (i.e., $V_{\text{bias}} = V_\pi$ or $b = \pi/2$), the optical carrier is suppressed as shown in Fig. 4(b). All of the even-order optical sidebands are eliminated so only the odd-order optical sidebands remain in the spectrum. Therefore, after square-law photodiode (PD) detection, a strong frequency-doubling millimeter-wave signal can be generated as the MZM is biased at either a maximum or minimum transmission point. In this paper, we will utilize this frequency-doubling modulation scheme with the MZM biased at a maximum or minimum transmission point to achieve frequency quadrupling without optical filtering.

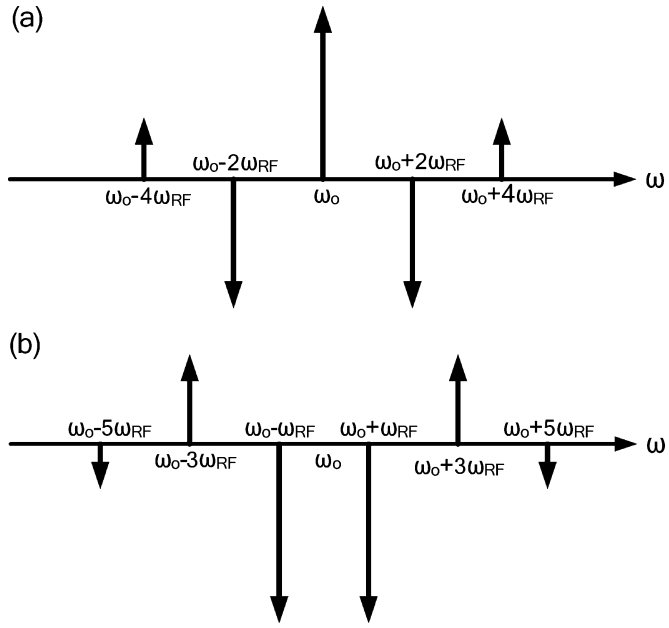

Fig. 4. Illustration of the optical spectrum using MZM biased at the: (a) maximum and (b) minimum transmission point.

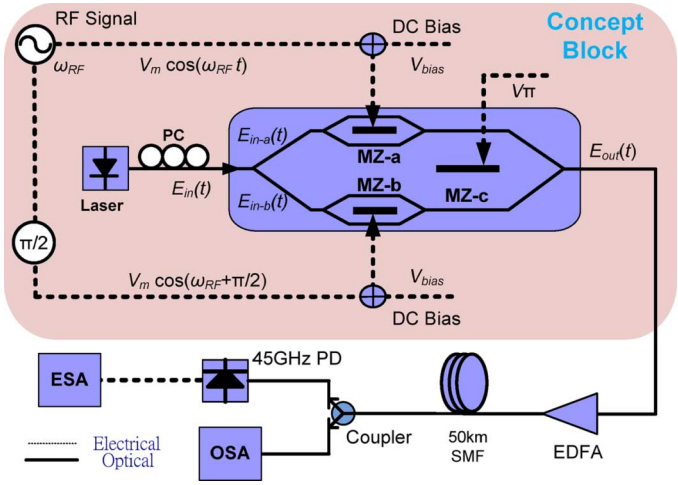

Fig. 5. Conceptual diagram and experimental setup of optical quadruple-frequency millimeter-wave signal generation using maximum transmission operation mode (polarization controller: PC, photodiode: PD, erbium-doped fiber amplifier: EDFA, optical spectrum analyzer: OSA, electrical spectrum analyzer: ESA).

B. Maximum Transmission Operation Mode

Fig. 5 shows a conceptual diagram of optical carrier-suppressed millimeter-wave signal generation using a frequency quadrupling technique with the MZM biased at the maximum transmission point [11]. An integrated MZM that is comprised of three sub-MZMs is key to generating optical millimeter-wave signals [14]. One sub-MZM (MZ-a or MZ-b) is embedded in each arm of the main modulator (MZ-c). The optical field at the input of the integrated MZM is defined as

$$E_{\text{in}}(t) = E_o \cos(\omega_o t). \tag{6}$$

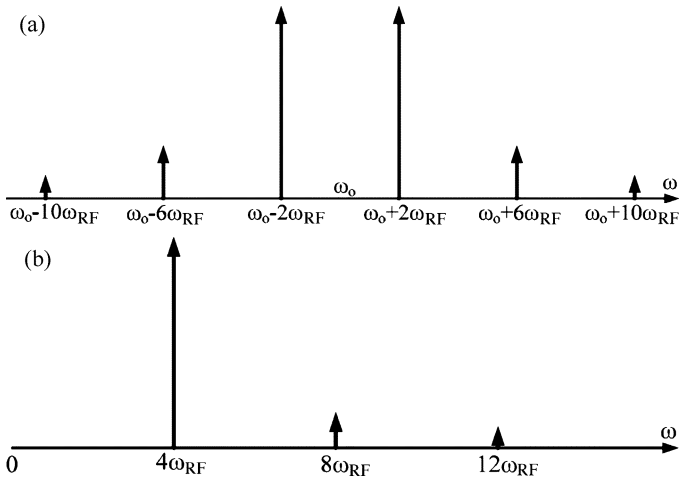

Fig. 6. (a) Illustrated spectrum of optical millimeter-wave signal using full-bias operation mode. (b) Illustrated spectrum of generated electrical millimeter-wave signal following square-law PD detection. Data from [14].

Both MZ-a and MZ-b are biased at the maximum transmission point. The electrical driving modulation signals sent into MZ-a and MZ-b are $V_a(t) = V_m \cos(\omega_{\text{RF}} t)$ and $V_b(t) = V_m \cos(\omega_{\text{RF}} t + (\pi/2))$, respectively. Moreover, the MZ-c is biased at the minimum transmission point. Therefore, the optical field at the output of the integrated MZM can be expressed as

$$E_{\text{out}}(t) = \frac{1}{2} \cdot E_o \cdot \cos(\omega_o t) \cdot \cos\left[m \cdot \cos(\omega_{\text{RF}} t)\right] - \cos(\omega_o t) \cdot \cos\left[m \cdot \cos\left(\omega_{\text{RF}} t + \frac{\pi}{2}\right)\right]. \tag{7}$$

Expanding $\cos[m \cdot \cos(\omega_{\text{RF}} t)]$ and $\cos[m \cdot \cos(\omega_{\text{RF}} t + (\pi/2))]$ using a Bessel function enables the output optical field to be rewritten as

$$E_{\text{out}}(t) = -E_o \sum_{n=1}^{\infty} J_{4n-2}(m) \cdot \{\cos\left[(\omega_o + (4n-2)\omega_{\text{RF}})\, t\right] + \cos\left[(\omega_o - (4n-2)\omega_{\text{RF}})\, t\right]\}. \tag{8}$$

Fig. 6(a) presents the optical spectrum of the generated millimeter-wave signal. Only optical sidebands with the second, sixth, and tenth orders are observed. Within the typical modulation range of $0 \le m \le \pi$, J_{4n-2} declines monotonically with m. When m is equal to π, the corresponding values of $J_2(m)$, $J_6(m)$, $J_{10}(m)$, and $J_{14}(m)$ are 0.4854, 0.0145, 2.0095×10^{-5}, and 5.4133 $\times$ 10^{-9}, respectively. Therefore, the optical sidebands with orders higher than J_6 can be neglected without significant errors, and the optical field can be further simplified to

$$E_{\text{out}}(t) = -E_o \{J_2(m) \cos\left[(\omega_o + 2\omega_{\text{RF}})t\right] + J_2(m) \cos\left[(\omega_o - 2\omega_{\text{RF}})t\right] + J_6(m) \cos\left[(\omega_o + 6\omega_{\text{RF}})t\right] + J_6(m) \cos\left[(\omega_o - 6\omega_{\text{RF}})t\right]\}. \tag{9}$$

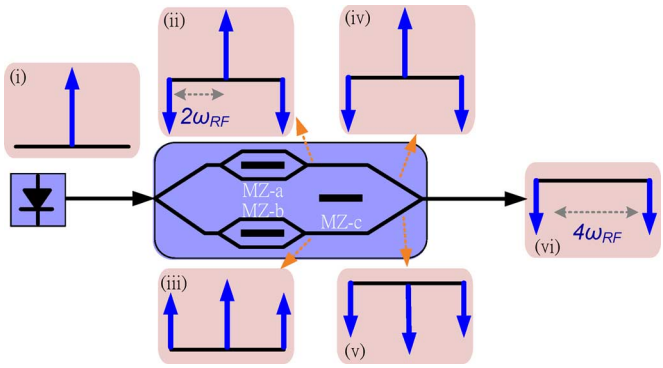

Fig. 7. Schematic principle of optical millimeter-wave generation using maximum transmission operation mode.

After square-law detection using a PD, the photocurrent can be expressed as

$$i(t) = R \cdot |E(t)|^2 \tag{10}$$

where R is the responsivity of a PD. The cross terms of (9) produce the desired millimeter-wave signal and its harmonic distortion signals. These millimeter-wave signal terms are

$$\begin{cases} i_{4\omega_{\mathrm{RF}}} = R \cdot E_o^2 \cdot [J_2(m) \cdot J_2(m) + 2 \cdot J_2(m) \cdot J_6(m)] \\ \qquad \cdot \cos(4\omega_{\mathrm{RF}} t) \\ i_{8\omega_{\mathrm{RF}}} = R \cdot E_o^2 \cdot [2 \cdot J_2(m) \cdot J_6(m)] \cdot \cos(8\omega_{\mathrm{RF}} t) \\ i_{12\omega_{\mathrm{RF}}} = R \cdot E_o^2 \cdot [J_6(m) \cdot J_6(m)] \cdot \cos(12\omega_{\mathrm{RF}} t). \end{cases} \tag{11}$$

Fig. 6(b) displays the electrical spectrum of the generated millimeter-wave signal after the square-law PD detection. Only the desired millimeter-wave signal $(4\omega_{\mathrm{RF}})$ and the harmonic distortion signals with frequency of $4n\omega_{\mathrm{RF}}$ are observed in the electrical spectrum, where n is an integer that exceeds two. Fig. 7 schematically depicts the principle of optical millimeter-wave generation using maximum transmission operation mode. Since MZ-a and MZ-b are biased at the maximum transmission point, the optical carrier and even-order sidebands are observed, as shown in insets (ii) and (iii) of Fig. 7. The optical sidebands with orders of more than two are neglected for simplicity. The 90° phase difference between the sinusoidal signals that drive MZ-a and MZ-b causes the polarities of the two second-order sidebands at the output of MZ-a to oppose those at the output of MZ-b. As the MZ-c is biased at the minimum transmission point, an extra 180° phase difference is added to all optical sidebands of the lower arms of MZ-c, as shown in insets (iv) and (v) of Fig. 7. Notably, the two optical carriers are out of phase, but the second-order sidebands are in phase. Therefore, after MZ-c, the optical carrier is eliminated and only two second-order sidebands remain, which can be converted into an electrical quadruple-frequency millimeter-wave signal following square-law PD detection.

C. Minimum Transmission Operation Mode

Fig. 8 presents the conceptual diagram of optical carrier-suppressed millimeter-wave signal generation using the same integrated MZM, but biased at the minimum transmission point. The electrical driving signals sent into the MZ-a and MZ-b are $V_a(t) = V_b(t) = V_m \cos(\omega_{\mathrm{RF}} t)$, and the electrical driving

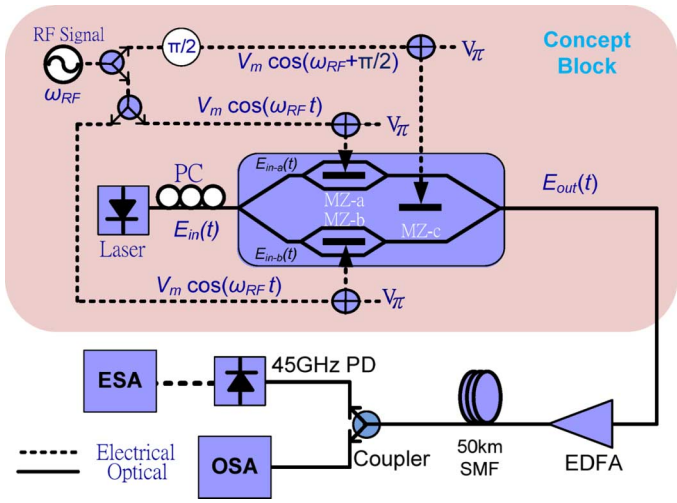

Fig. 8. Conceptual diagram and experimental setup of optical quadruple-frequency millimeter-wave signal generation using minimum transmission operation mode (polarization controller: PC, photodiode: PD, erbium-doped fiber amplifier: EDFA, optical spectrum analyzer: OSA, electrical spectrum analyzer: ESA).

signal for MZ-c is $V_c(t) = V_m \cos(\omega_{\mathrm{RF}} t + (\pi/2))$. Therefore, the optical field at the output of the integrated MZM is given by

$$E_{\mathrm{out}} = -E_o \cdot \sin[m \cdot \cos(\omega_{\mathrm{RF}} t)] \cdot \sin[m \cdot \sin(\omega_{\mathrm{RF}} t)] \cdot \cos(\omega_o t). \tag{12}$$

Expanding $\sin[m \cdot \cos(\omega_{\mathrm{RF}} t)]$ and $\sin[m \cdot \sin(\omega_{\mathrm{RF}} t)]$ using the Bessel functions enables the output optical field to be rewritten as

$$\begin{aligned} E_{\mathrm{out}} = E_o \sum_{k=0}^{\infty} \Bigg[\Bigg\{ \Bigg[\sum_{a=1}^{2k+1} (-1)^{a-1} \cdot J_{2a-1}(m) \\ \cdot J_{(4k+2)-(2a-1)}(m) \Bigg] \\ + \Bigg[2 \cdot \sum_{b=1}^{\infty} (-1)^{b-1} \cdot J_{2b-1}(m) \\ \cdot J_{(2b-1)+(4k+2)}(m) \Bigg] \Bigg\} \\ \cdot \{ \sin[(\omega_o - (4k+2)\omega_{\mathrm{RF}}) \cdot t] \\ - \sin[(\omega_o + (4k+2)\omega_{\mathrm{RF}}) \cdot t] \} \Bigg]. \end{aligned} \tag{13}$$

Fig. 9(a) shows that only optical sidebands with the second, sixth, and tenth orders are observed. Without causing significant errors, the Bessel function with the order higher than J_3 are ignored, and the optical field can be further simplified to

$$\begin{aligned} E_{\mathrm{out}} = E_o \Big\{ & [J_1(m) \cdot J_1(m) + 2 \cdot J_1(m) \cdot J_3(m)] \\ & \cdot \sin[(\omega_o - 2\omega_{\mathrm{RF}})t] \\ & - [J_1(m) \cdot J_1(m) + 2 \cdot J_1(m) \cdot J_3(m)] \\ & \cdot \sin[(\omega_o + 2\omega_{\mathrm{RF}})t] + [-J_3(m) \cdot J_3(m)] \\ & \cdot \sin[(\omega_o - 6\omega_{\mathrm{RF}})t] - [-J_3(m) \cdot J_3(m)] \\ & \cdot \sin[(\omega_o + 6\omega_{\mathrm{RF}})t] \Big\}. \end{aligned} \tag{14}$$

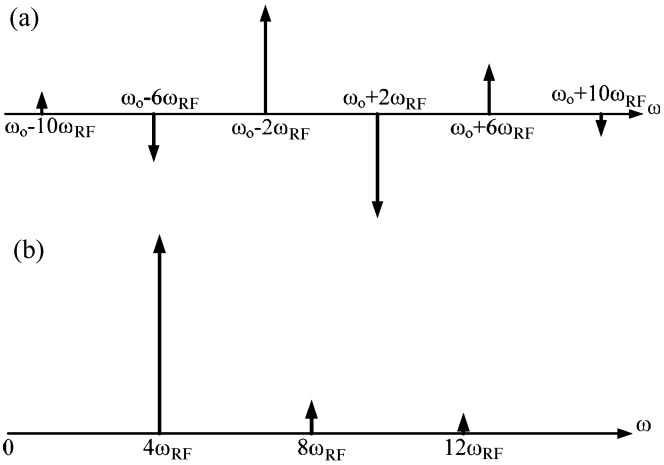

Fig. 9. (a) Illustrated spectrum of optical millimeter-wave signal using null-bias operation mode. (b) Illustrated spectrum of generated electrical millimeter-wave signal following square-law PD detection.

After square-law PD detection, the desired millimeter-wave signal and its harmonics distortion signals are

$$\begin{aligned} i_{4\omega_{\mathrm{RF}}} &= R \cdot E_o^2 \cdot \left[-J_1^4(m) - 4 \cdot J_1^3(m) \cdot J_3(m) \right. \\ &\quad \left. -6 \cdot J_1^2(m) \cdot J_3^2(m) - 4 \cdot J_1(m) \cdot J_3^3(m)\right] \\ &\quad \cdot \cos(4\omega_{\mathrm{RF}} t) \\ i_{8\omega_{\mathrm{RF}}} &= R \cdot E_o^2 \cdot \left[2 \cdot J_1^2(m) \cdot J_3^2(m) + 4 \cdot J_1(m) \cdot J_3^3(m)\right] \\ &\quad \cdot \cos(8\omega_{\mathrm{RF}} t) \\ i_{12\omega_{\mathrm{RF}}} &= R \cdot E_o^2 \cdot \left[-J_3^4(m)\right] \cdot \cos(12\omega_{\mathrm{RF}} t). \end{aligned} \tag{15}$$

Fig. 9(b) presents the electrical spectrum of the millimeter-wave signal following square-law PD detection. The result obtained using the minimum transmission operation mode is the same as that obtained using the maximum transmission operation mode, and only the desired millimeter-wave signal $(4\omega_{\mathrm{RF}})$ and the harmonic distortion signals with frequencies of $4n\omega_{\mathrm{RF}}$ are observed in the electrical spectrum, where n is an integer that is larger than two.

Fig. 10 schematically depicts the principle of optical millimeter-wave generation using the minimum transmission operation mode. When MZ-a and MZ-b are biased at the minimum transmission point, two first-order sidebands with carrier suppression are generated and the optical sidebands with orders of more than two are neglected for simplicity. Since no phase difference exists between two driving signals for MZ-a and MZ-b, the polarities of optical sidebands at the output of MZ-a and MZ-b are identical, as presented in insets (ii) and (iii) of Fig. 10. These two identical two-tone lightwaves at the output of MZ-a and MZ-b can be regarded as two coherent lightwave sources before MZ-c. When an electrical signal $V_c(t)$ with a 90° phase delay, which is relative to $V_a(t)$ and $V_b(t)$, is applied at MZ-c, each lighwave generates two first-order sidebands with optical carrier suppression, and an extra $+90°$ and $-90°$ phase differences are added to the upper and lower sidebands, respectively. As presented in inset (iv) of Fig. 10, the polarities of the two generated optical sidebands at the original carrier frequency oppose each other. Accordingly, two second-order sidebands with carrier suppression are obtained and can be converted into a quadruple-frequency electrical millimeter-wave signal following square-law PD detection.

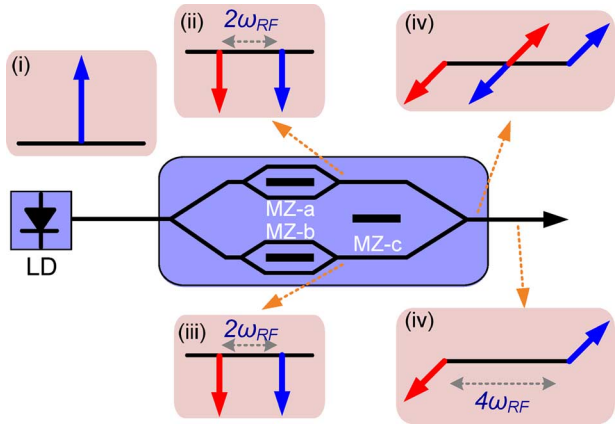

Fig. 10. Schematic principle of optical millimeter-wave generation using minimum transmission operation mode.

III. Experimental Verification of Two Proposed Methods

To verify these two proposed methods, experiment setups using maximum and minimum transmission operation modes are performed as displayed in Figs. 5 and 8, respectively. The external integrated MZM is a commercially available $LiNbO_3$ modulator. A commercial distributed feedback laser is employed as a light source and a polarization controller is adopted to adjust the polarization before the light is sent into the modulator. The frequency of the driving signal is set at 10, 15, and 18 GHz, respectively. The generated optical millimeter-wave signal is amplified using an erbium-doped fiber amplifier to compensate the loss of the integrated MZM and then transmitted with launch power of 0 dBm over a 50-km single-mode fiber. The optical power is normalized to 1 dBm before PD detection. Both optical and electrical spectra of millimeter-wave signals using maximum and minimum transmission operation modes are experimentally investigated.

A. Maximum Transmission Operation Mode

Fig. 11(a) shows the measured spectrum of the optical 40-GHz millimeter-wave signal using a 10-GHz driving signal before transmission. The optical carrier is effectively suppressed, and the power of the two second-order sidebands, which can be converted into a 40-GHz electrical millimeter-wave signal after PD detection, is 38 dB higher than that of the other order sidebands. Sidebands other than the second- and sixth-order sidebands are observed due to the imbalance in the y-junction splitting ratio of MZM. The suppression of the undesired harmonic sidebands exceeds 38 dB and negligibly affects the performance of the optical millimeter-wave signal. Fig. 11(b) presents the waveform of the optical millimeter-wave signal with a 50% duty cycle associated with a high OCHDSR of more than 38 dB.

Fig. 12 presents the electrical spectrum of the generated back-to-back millimeter-wave signal with a 40-GHz span and 30-kHz resolution bandwidth. A strong electrical signal with

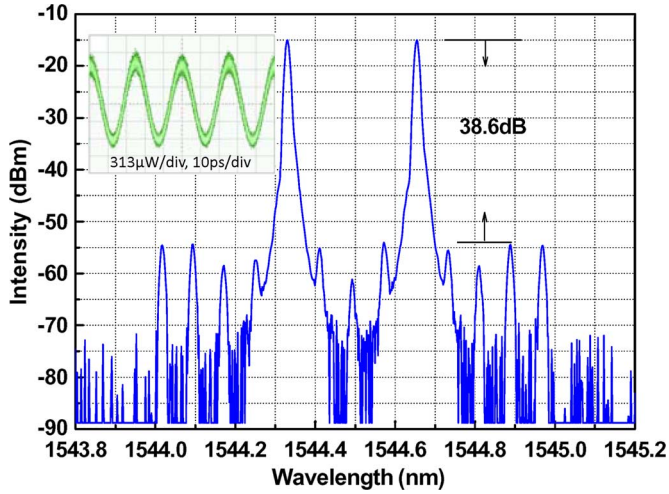

Fig. 11. Experimental results of 40-GHz optical millimeter-wave signal spectrum using maximum transmission operation mode. The resolution is 0.01 nm.

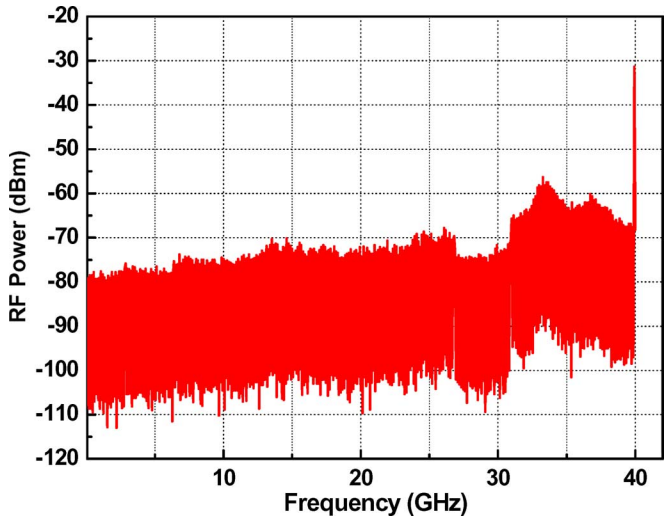

Fig 12. Measured electrical spectrum of the generated back-to-back 40-GHz millimeter-wave signal using maximum transmission operation mode.

the frequency four times the driving signal is observed, and the first, second, and third terms of the electrical signal are totally suppressed below the noise floor. Since the suppression of the undesired harmonic sidebands is more than 38 dB, there is no observable change following 50-km single-mode fiber transmission, and the spectrum remains very clear with the same suppression ratio, as presented in Fig. 12. Fig. 13(a) reveals that the linewidth of the generated 40-GHz signal is less than 5 Hz and almost equals to that of the 10-GHz driving signal. After transmission over the 50-km single-mode fiber, no linewidth broadening of the electrical 40-GHz signal due to fiber dispersion is observed, as shown in Fig. 13(b). Due to the available RF amplifier in the authors' laboratory, only 72-GHz millimeter-wave signals are obtained by using a 18-GHz electrical driving signal, respectively. Fig. 14 shows that the optical powers of the two desired second-order sidebands of millimeter-wave signals are at least 36 dB higher than those of the other sidebands, which suffices for most practical application.

Minimum Transmission Operation Mode: Fig. 15(a) shows the spectrum of the optical back-to-back 40-GHz millimeter-

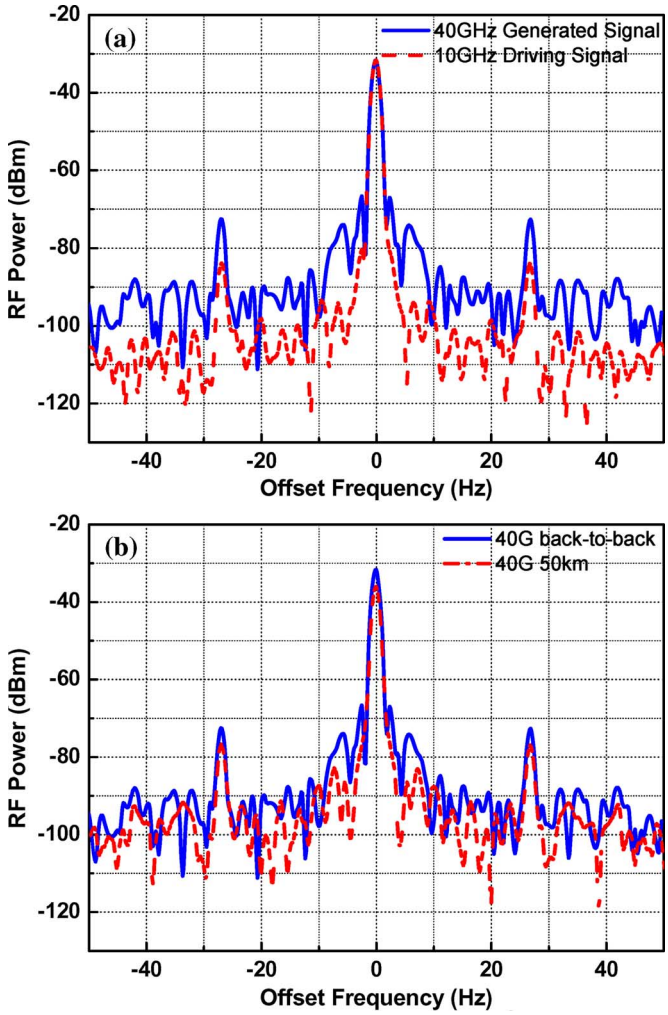

Fig 13. Measured electrical spectrum of the generated 40-GHz millimeter-wave signal using maximum transmission operation mode with 100-Hz span. (a) Comparison of generated 40-GHz signal and 10-GHz driving signal. (b) Comparison of generated back-to-back and following 50-km single-mode fiber transmission 40-GHz signal. The resolution bandwidth is 1 Hz.

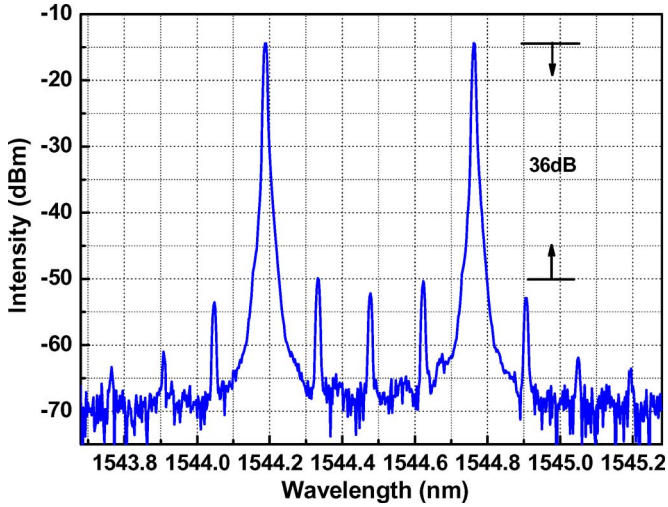

Fig. 14. Measured optical spectrum of the generated 72-GHz millimeter-wave signals using 18-GHz driving signals, respectively.

wave signal obtained using a minimum transmission operation mode. The suppression ratio of the optical carrier and undesired

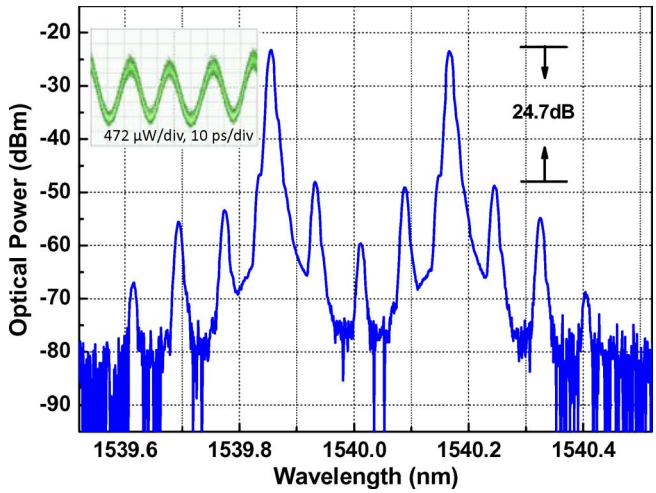

Fig. 15. Experimental results of 40-GHz optical millimeter-wave signal spectrum using minimum transmission operation mode. The resolution is 0.01 nm.

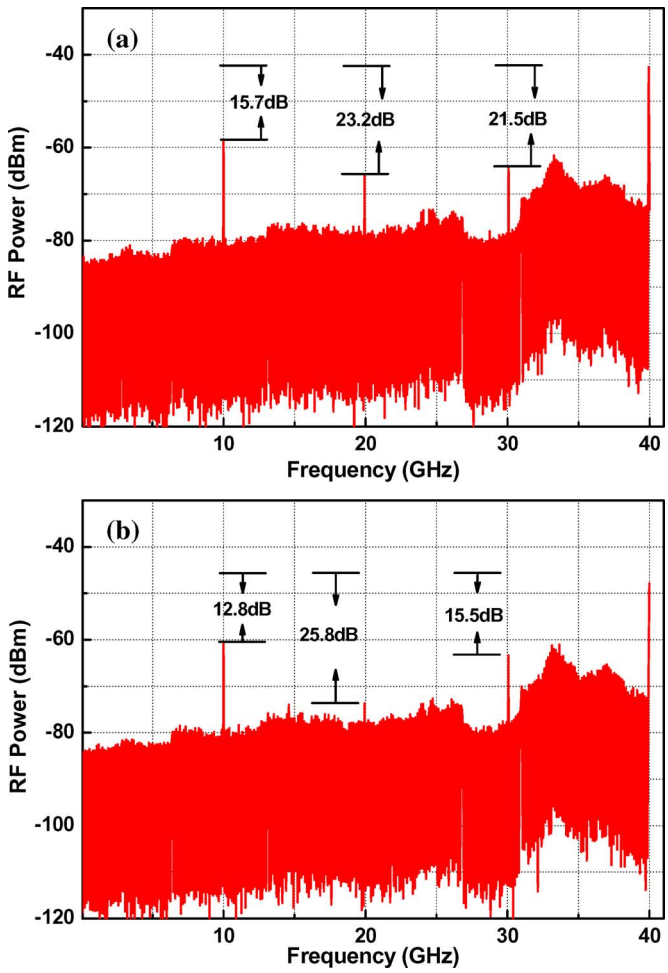

Fig. 16. Measured electrical spectrum of the generated 40-GHz millimeter-wave signal using minimum transmission operation mode. (a) Back to back. (b) Following 50-km single-mode fiber transmission.

harmonic distortions exceeds 24 dB. Although the duty cycle of optical millimeter-wave signal is close to 50%, the limited suppression ratio slightly blurs the envelope of the optical millimeter-wave signal waveform. Fig. 16 presents the electrical

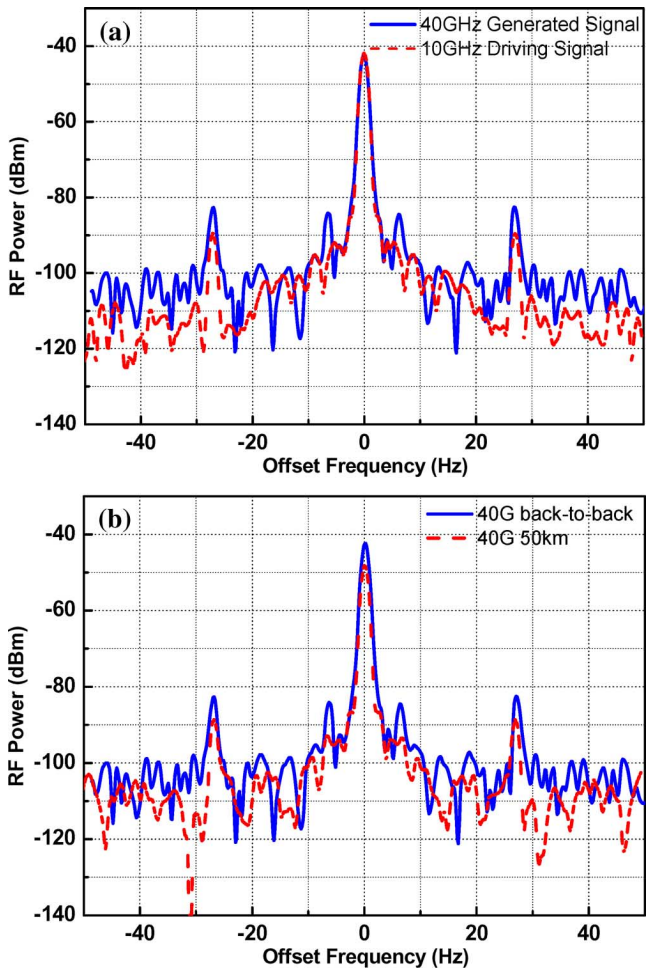

Fig. 17. Measured electrical spectrum of the generated 40-GHz millimeter-wave signal using minimum transmission operation mode with 100-Hz span. (a) Comparison of generated 40-GHz signal and 10-GHz driving signal. (b) Comparison of generated back-to-back and following 50-km single-mode fiber transmission 40-GHz signal. The resolution bandwidth is 1 Hz.

spectrum of the generated 40-GHz millimeter-wave signal. Not only a quadruple-frequency electrical signal is observed, but also the first, second, and third harmonic terms of the electrical signal are observed. Additionally, the undesired electrical distortion suppression ratio declines from 15.7 to 12.8 dB after 50-km single-mode fiber transmission. Fig. 17(a) reveals that the linewidth of the generated 40-GHz signal is almost equal to that of the 10-GHz driving signal. Following transmission over the 50-km single-mode fiber, no linewidth broadening of the electrical 40-GHz signal due to fiber dispersion is observed, as presented in Fig. 17(b). Fig. 18 shows that the OCHDSRs of the 72-GHz millimeter-wave signal can exceed 22 dB.

IV. Comparison

For an ideally balanced MZM, regardless of which proposed method is adopted, only the optical sidebands of the order $\pm(4n-2)$ are observed, as evident in (8) and (13). However, the imbalance of the two arms of the MZM produces other undesired optical sidebands. The OCHDSRs obtained using a maximum transmission operation mode markedly exceeds those obtained using a minimum transmission operation mode,

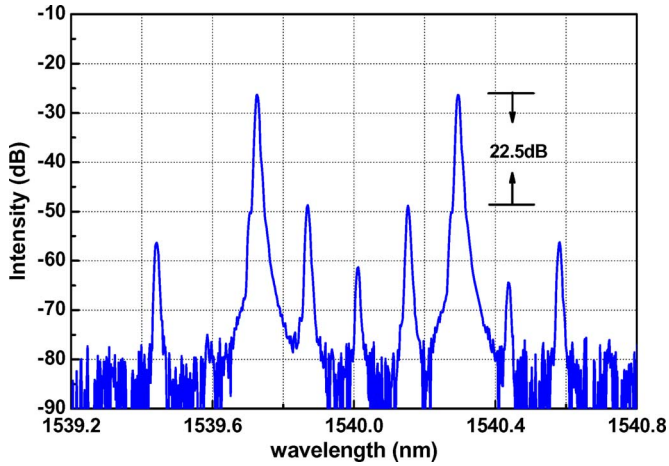

Fig. 18. Measured optical spectrum of the generated 72-GHz millimeter-wave signal using 18-GHz driving signal.

as displayed in Figs. 11, 14, 15, and 18. For the maximum transmission operation mode, the active trimming approach, i.e., adjusting the bias points and the amplitudes of the driving signals for MZ-a and MZ-b, can be used to compensate for the MZM imbalance. Therefore, higher OCHDSRs can be obtained, as has been demonstrated elsewhere [13]. For minimum transmission operation mode, the two first-order sidebands dominate the suppression ratio, as presented in Figs. 15 and 18. Two main sources are responsible for the undesired first-order sideband. The first source is the amplitude imbalance of MZ-a and MZ-b. With MZ-a and MZ-b biased at the minimum transmission point, the generated double-frequency millimeter-wave signal using a balanced MZM have an infinite optical carrier suppression ratio. Due to fabrication errors, a perfectly balanced MZM is difficult to achieve. Therefore, the residual optical carrier caused by MZ-a and MZ-b imbalances will contribute to the two first-order sidebands after MZ-c modulation. The second source is the MZ-c imbalance. The two first-order sidebands generated by MZ-a and MZ-b are regarded as two coherent lightwave sources before MZ-c modulation. The suppression ratio of those two first-order sidebands depends on the amplitude imbalance of the MZ-c at the output of the integrated MZM. Therefore, the imbalances of the three sub-MZMs dominates the OCHDSR of the quadruple-frequency millimeter-wave signal when the minimum transmission operation mode is used, and active trimming cannot be adopted to eliminate the imbalance.

Notably, the amplitudes of the two desired second-order sidebands of optical millimeter-wave signals obtained using maximum and minimum transmission operation mode are related mostly to the second- and first-order Bessel function, respectively. When $0 \leq m \leq \pi$, $J_1(m)$ is larger than $J_2(m)$. To achieve high OCHDSRs, the modulation index (MI) $= V_m/2V_\pi = m/\pi$) for a driving integrated MZM using a maximum transmission operation mode exceeds that obtained using a minimum transmission operation mode. For a maximum transmission operation mode, the optimal MI for maximum OCHDSRs, which is determined by the MZM imbalance, ranges from 1.2 to 1.8. Hence, a narrowband RF high power amplifier for a driving MZM or z-cut integrated MZM (i.e., two-electrode MZ-a and MZ-b) [13] is required for the maximum transmission operation mode. For the minimum transmission operation mode, the optimal MI is less than 0.7. Therefore, only an RF medium power amplifier or x-cut integrated MZM (i.e., single electrode MZ-a, MZ-b, and MZ-c) is needed.

V. Conclusions

This paper has presented two novel frequency quadrupling techniques for optical millimeter-wave generation. A two-tone lightwave with a frequency separation four times of the modulation frequency can be generated using only one external modulator without optical filtering. The OCHDSRs of these optical millimeter-wave signals obtained using a maximum and minimum transmission operation mode can exceed 36 and 22 dB, respectively, which values suffice for most applications. Since no optical filter is needed, the proposed approaches can be adopted for optical up-conversion in WDM RoF systems and continuously tunable millimeter-wave signal systems. Since the state-of-the-art MZM has an upper-limit frequency response of about 40 GHz [13], the two proposed methods can generate optical millimeter-wave signals up to 160 GHz.

References

[1] X. Wei, J. Leuthold, and L. Zhang, "Delay-interferometer-based optical pulse generator," presented at the Proc. Opt. Fiber Commun. Conf., 2004, Paper WL6.

[2] G. Qi, J. Yao, S. Joe, S. Paquet, and C. Belisle, "Optical generation and distribution of continuously tunable millimeter-wave signals using an optical phase modulator," *J. Lightw. Technol.*, vol. 23, no. 9, pp. 2687–2695, Sep. 2005.

[3] G. Qi, J. Yao, J. Seregelyi, S. Paquet, and C. Belisle, "Generation and distribution of a wide-band continuously tunable millimeter-wave signal with an optical external modulation technique," *IEEE Trans. Microw. Theory Tech.*, vol. 53, no. 10, pp. 3090–3097, Oct. 2005.

[4] A. Wiberg, P. Perez-Millan, M. V. Andres, and P. O. Hedekvist, "Microwave-photonic frequency multiplication utilizing optical four-wave mixing and fiber bragg gratings," *J. Lightw. Technol.*, vol. 24, no. 1, pp. 329–334, Jan. 2006.

[5] Q. Wang, H. Rideout, F. Zeng, and J. Yao, "Millimeter-wave frequency tripling based on four-wave mixing in a semiconductor optical amplifier," *IEEE Photon. Technol. Lett.*, vol. 18, no. 12, pp. 2460–2462, Dec. 2006.

[6] Z. Pan, S. Chandel, and C. Yu, "160 GHz optical pulse generation using a 40 GHz phase modulator and two stages of delayed MZ interferometers," presented at the Proc. Lasers Electro-Opt. Conf., 2006, Paper CFP2.

[7] C. Yu, Z. Pan, T. Luo, T. Wang, L. Christen, and A. E. Willner, "Beyond 40-GHz return-to-zero optical pulse-train generation using a phase modulator and polarization-maintaining fiber," *IEEE Photon. Technol. Lett.*, vol. 19, no. 1, pp. 42–44, Jan. 2007.

[8] M. Mohamed, X. Zhang, B. Hraimell, and K. Wu, "Frequency sixupler for millimeter-wave over fiber systems," *Opt. Exp.*, vol. 16, no. 14, pp. 10141–10151, Jul. 2008.

[9] M. Mohamed, X. Zhang, B. Hraimell, and K. Wu, "Analysis of frequency quadrupling using a single Mach–Zehnder modulator for millimeter-wave generation and distribution over fiber systems," *Opt. Exp.*, vol. 16, no. 14, pp. 16786–16802, Jul. 2008.

[10] Z. Xu, X. Zhang, and J. Yu, "Frequency upconversion of multiple RF signals using optical carrier suppression for radio over fiber downlinks," *Opt. Exp.*, vol. 15, no. 25, pp. 16737–16747, Dec. 2007.

[11] J. Yu, Z. Jia, L. Yi, G. K. Chang, and T. Wang, "Optical millimeter-wave generation or up-conversion using external modulator," *IEEE Photon. Technol. Lett.*, vol. 18, no. 1, pp. 265–267, Jan. 2006.

[12] J. Kondo, K. Aoki, Y. Iwata, A. Hamajima, T. Ejiri, O. Mitomi, and M. Minakata, "76-GHz millimeter-wave generation using MZ LiNbO3 modulator with drive voltage of 7 Vp-p and 19 GHz signal input," *J. Lightw. Technol.*, vol. 24, no. 1, pp. 329–334, Jan. 2006.

[13] T. Kawanishi, T. Sakamoto, and M. Izutsu, "High-speed control of lightwave amplitude, phase, and frequency by use of electrooptic effect," *IEEE J. Sel. Topics Quantum Electron.*, vol. 13, no. 1, pp. 79–90, Jan./Feb. 2007.

[14] C.-T. Lin, P. T. Shih, J. Chen, P.-C. Peng, S.-P. Dai, W.-Q. Xue, and S. Chi, "Generation of carrier suppressed optical mm-wave signals using frequency quadrupling and no optical filtering," presented at the Opt. Fiber Commun. Conf., 2008, Paper JThA 73.

Chun-Ting Lin received the B.S. and M.S. degrees in material science and engineering from National Tsing Huang University, Hsinchu, Taiwan, in 1997 and 2001, respectively, and the Ph.D. degree in electro-optical engineering from National Chiao-Tung University, Hsinchu, Taiwan, in 2007.

From 2007 to 2009, he was a Research Associate with the Department of Photonics, National Chiao Tung University, Hsinchu, Taiwan. In 2009, he joined the faculty of National Chiao Tung University, where he is currently an Assistant Professor with the Institute of Photonic System, College of Photonics National Chiao Tung University at Tainan, Taiwan. His research interests are RoF systems, optical millimeter/sub-terahertz wave generation and application, optical data formats, and opto-electronic packages.

Po-Tsung Shih received the B.S. and M.S. degree in electrophysics from National Chiao Tung University (NCTU), Hsinchu, Taiwan, in 2004 and 2006, respectively, and is currently working toward the Ph.D. degree at the Institute of Electro-Optical Engineering, NCTU.

His research interests are RoF systems, optical millimeter-wave generation, optical data formats, and optical access networks.

Jason (Jyehong) Chen received the B.S. and M.S. degrees in electrical engineering from National Taiwan University, Taiwan, in 1988 and 1990, respectively, and the Ph.D. degree in electrical engineering and computer science from the University of Maryland Baltimore County, Baltimore, in 1998.

In 1998, he joined the JDSU Uniphase Corporation, as a Senior Engineer. In 2003, he joined the faculty of National Chiao Tung University, Hsinchu, Taiwan, where he is currently an Associate Professor with the Institute of Electro-Optical Engineering and the Department of Photonics. He holds ten U.S. patents (earned within a two-year period).

Wen-Jr Jiang received the B.S. degree in electrophysics and M.S. degree in display from the Institute of Electro-Optical Engineering, National Chiao Tung University (NCTU), Hsinchu, Taiwan, in 2006 and 2008, respectively, and is currently working toward the Ph.D. degree at the Institute of Electro-Optical Engineering, NCTU.

His research interests are RoF systems, optical millimeter-wave generation, photonic vector signal generation, and hybrid access networks.

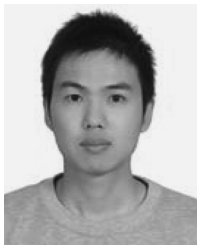

Sheng-Peng Dai received the B.S. degree in electrical engineering from National Taipei University of Technology (NTUT), Taipei, Taiwan, in 2006, and is currently working toward the M.S. degree at the Institute of Electro-Optical Engineering, National Chiao Tung University (NCTU).

His research interests include orthogonal frequency-division multiplexing (OFDM) in RoF and optical access networks.

Peng-Chun Peng received the Ph.D. degree from the Institute of Electro-Optical Engineering, National Chiao Tung University, Taiwan, in 2005.

From 2006 to 2008, he was an Assistant Professor with the Department of Applied Materials and Optoelectronic Engineering and the Department of Electrical Engineering, National Chi Nan University, Taiwan. In 2008, he joined the Department of Electro-Optical Engineering, National Taipei University of Technology, Taiwan, as an Assistant Professor. His research interests include optical communication systems, vertical-cavity surface-emitting lasers, fiber sensors, optical signal processing, and microwave photonics.

Yen-Lin Ho was born in TaoYuan, Taiwan, on March 30, 1985. He received the B.S. degree in electro-optical engineering from National Chiao Tung University (NCTU), Taiwan, in 2008, and is currently working toward the M.S. degree at the Institute of Electro-Optical Engineering, NCTU.

Sien Chi received the B.S.E.E. degree from National Taiwan University, Taipei, Taiwan, in 1959, the M.S.E.E. degree from National Chiao-Tung University, Hsinchu, Taiwan, in 1961, and the Ph.D. degree in electro-physics from the Polytechnic Institute, Brooklyn, NY, in 1971.

From 1971 to 2004, he was a Professor with National Chiao-Tung University. From 1998 to 2001, he was the Vice President of National Chiao-Tung University. He is currently a Chair Professor with Yuan-Ze University, Chung Li, Taiwan. His research interests are optical-fiber communications, optical solitons, optical modulation formats, and optical-fiber amplifiers.

Dr. Chi is a Fellow of the Optical Society of America (OSA).